LATERAL FORCE RESISTING MECHANISMS IN SLAB-COLUMN CONNECTIONS: AN ANALYTICAL APPROACH

Ioannis-Sokratis DRAKATOS[1], Katrin BEYER[2] and Aurelio MUTTONI[3]

ABSTRACT

In many countries reinforced concrete (RC) flat slabs supported on columns is one of the most commonly used structural systems for office and industrial buildings. To increase the lateral stiffness and strength of the structure, RC walls are typically added and carry the largest portion of the horizontal loads generated during earthquakes. While the slab-column system is typically not relevant with regard to the lateral stiffness and strength of the structure, each slab-column connection has to have the capacity to follow the seismically induced lateral displacements of the building while maintaining its capacity to transfer vertical loads from the slab to the columns. If this is not the case, brittle punching failure of the slab occurs and the deformation capacity of the entire building is limited by the deformation capacity of the slab-column connection. This article presents an analytical approach for predicting the moment resistance of all mechanisms that contribute to the strength of the slab-column connection when subjected to earthquake-induced drifts. The approach is based on the Critical Shear Crack Theory (CSCT). The performance of the model is verified comparing the analytical predictions with experiments from the literature. The influence of gravity induced loads on the flexural behaviour of slab-column connections under seismic loading as well as the contribution of the various resistance-providing mechanisms for increasing drifts are discussed.

INTRODUCTION

Reinforced concrete (RC) flat slabs supported on columns offers several advantages for office and industrial building construction, such as large open spaces and short construction times. Due to the low horizontal stiffness of the structure, vertical spines (shear and/or core walls) are added in seismic prone areas to carry the largest portion of the horizontal loads generated during earthquakes. Although the slab-column system is not part of the lateral force resisting system of the structure, each slab-column connection has to have the capacity to follow the seismically induced lateral displacements of the building while maintaining its capacity to transfer vertical loads from the slab to the columns. Otherwise brittle punching failure of the slab occurs and the deformation capacity of the connection determines the deformation capacity of the entire building.

---

[1] M.Sc., Structural Concrete Laboratory (IBETON), School of Architectural, Civil and Environmental Engineering (ENAC), Ecole Polytechnique Fédérale de Lausanne, Lausanne, ioannis-sokratis.drakatos@epfl.ch
[2] Assistant Professor, Earthquake Engineering and Structural Dynamics Laboratory (EESD), School of Architectural, Civil and Environmental Engineering (ENAC), Ecole Polytechnique Fédérale de Lausanne, Lausanne, katrin.beyer@epfl.ch
[3] Professor, Structural Concrete Laboratory (IBETON), School of Architectural, Civil and Environmental Engineering (ENAC), Ecole Polytechnique Fédérale de Lausanne, Lausanne, aurelio.muttoni@epfl.ch

When a slab-column connection is subjected to a combination of moment and shear force and is responding in the elastic range, three different mechanisms are contributing to the moment resistance (Fig.1a): (i) shear force eccentric to the column axis, (ii) flexure and (iii) torsion. As the behaviour of the slab-column connection subjected to an eccentric moment becomes non-linear—even if this nonlinearity results only from cracking—an accurate and realistic estimation of the contribution of the resisting mechanisms to the overall capacity of the slab-column connection is rather difficult. This is accentuated by the fact that the aforementioned resistance mechanisms are associated with different failure modes.

Several researchers investigated the contribution of the different mechanisms to the overall resistance of the slab-column connection. The common experimental approach for estimating the contribution of flexure and torsion mechanisms consists in cutting slots in the slab in the proximity of the column faces (Hanson and Hanson, 1968). Other researchers (Kanoh and Yoshizaki, 1979) applied a force couple to a column connected monolithically to the slab specimen at only one column-slab interface so that only torsion is tranferred from the column to the slab.

Although experimental evidence on the different contributions of the resisting mechanisms is limited, the design equations in codes of practice (ACI 318, 2011; Eurocode 2, 2004) are based on estimating the contribution of the eccentric shear and bending moment mechanisms on the basis of empirical works while neglecting the contribution of the torsion mechanism. Another important assumption of these equations is the fact that the distribution of shear stresses on the critical perimeter is linear according to ACI 318 (2011) or uniform according to Eurocode 2 (2004) as shown in Fig.1b. As a result, due to the nonlinear distribution of shear stresses on the control perimeter and depending on the actual contribution of the resistance-providing mechanisms at failure the code equations underpredict / overpredict the moment capacity of slab-column connections. Furthermore, a generally accepted method for calculating the moment that is transferred to the connection and a model for capturing the relationship between moment and deformation capacity are lacking.
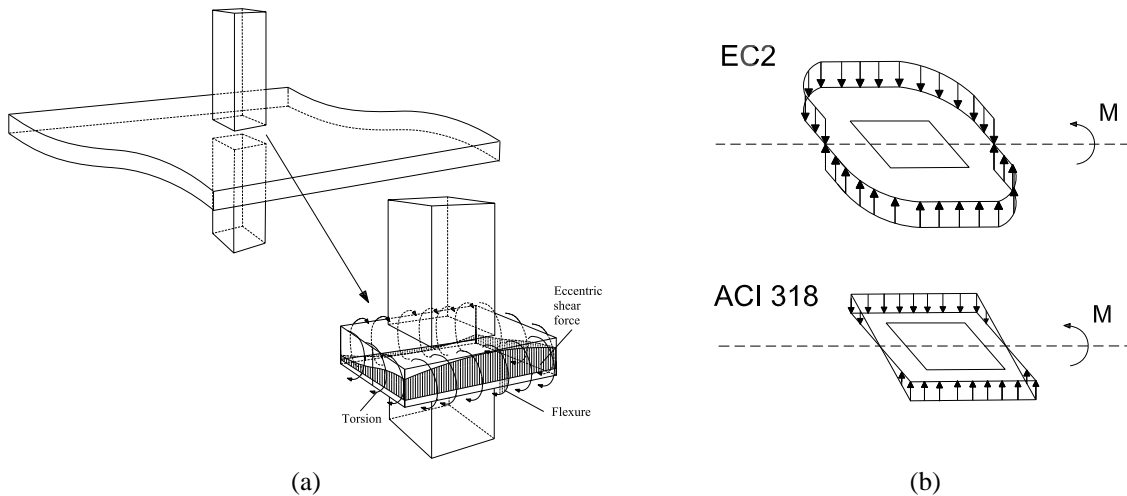

Figure 1. (a) Internal forces in the vicinity of the column for vertical loading and inserted moment due to earthquake-type loading according to the theory of elasticity, and (b) assumed distribution of shear stresses in the control perimeter according to Eurocode 2 (2004) and ACI 318 (2011)

In order to design and assess buildings with flat slabs and columns for seismically induced drifts, the estimation of the moment-rotation relationship of slab-column connections including the rotation capacity are essential. A model for predicting the moment-rotation relationship should capture the size effect, the gravity load effect, the influence of column size and the influence of the reinforcement ratio. Moreover, as punching is a brittle local failure due to excessive shear stresses in the proximity of the slab-column connection, the need for a relationship between local rotations and global interstory drift ψ_{st} becomes obvious (Fig.2).

This article presents an analytical model for predicting the contribution of all resistance-providing mechanisms for slab-column connections subjected to earthquake-induced drifts (Fig.2), considering both the load and the deformation of the slab. The model is based on the Critical Shear Crack Theory (Muttoni, 2008) which has been employed successfully for predicting the flexural

behaviour of slab-column connections for gravity induced loads considering both the load and the deformation and which forms the basis of the punching shear equations of the FIB Model Code (2010). The contribution of the different resistance-providing mechanisms is obtained by means of formulating equilibrium equations for a slab sector when a moment due to seismically induced drifts is applied to the slab-column connection.
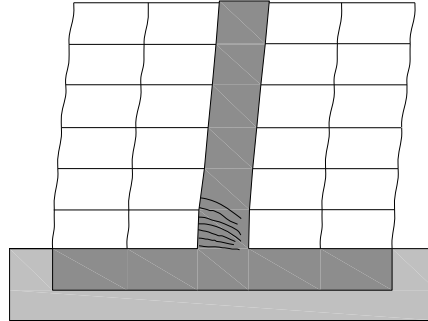

Figure 2. Deformation state of slab-column connections at global level for seismically induced drifts

The analytical approach is compared to experimental results from the literature to verify whether the influence of gravity loads on the flexural behaviour is effectively captured. Comparisons with respect to the reinforcement ratio and eccentricity influence can be found elsewhere (Drakatos et al., 2014). The contribution of the different resisting mechanisms for increasing values of lateral deformations is also discussed.

ANALYTICAL MODEL

The theoretical background of the proposed model is presented hereafter focusing in particular on the modifications introduced when compared to the CSCT. The load is assumed to be transferred to the column through an inclined compression strut. The presence of a critical shear crack that propagates along this strut reduces the shear strength of the connection (Muttoni, 2008). Therefore, the slab is divided into n sector elements and the region inside the shear crack. The difference when compared to the CSCT is the fact that the state of rotations is not the same for all the sector elements. Consequently torsional moments and moments due to eccentric shear force are introduced in the connection in addition to the moments due to flexure. The kinematic assumption and curvature distributions are shown in Fig.3. The equilibrium principles on the local level are illustrated in Fig.4. The half of the slab where the transferred moment increases the deflection of the slab due to vertical loads is denoted as "negative slab half" (negative moment due to seismic loading), whereas the other half where tension in the bottom reinforcement may appear is denoted as "positive slab half" (positive moment due to seismic loading).
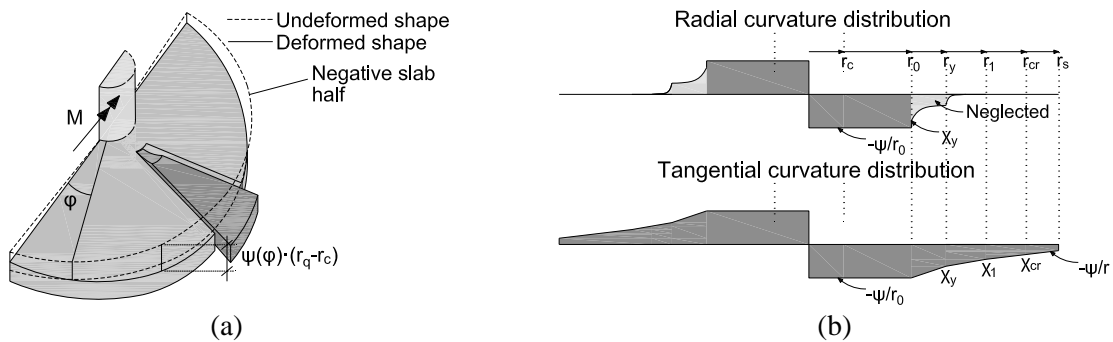

Figure 3. Proposed mechanical model: (a) kinematic assumption for the rotations of the sector elements (negative slab half), and (b) distribution of radial and tangential curvatures along the diameter of the isolated slab element (for upwards deflection of the positive slab half)
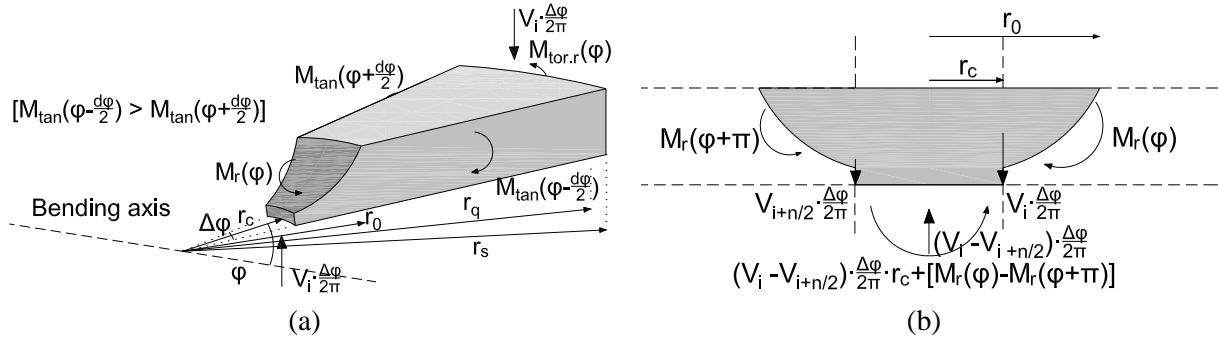
Figure 4. Internal forces acting on the slab region: (a) outside the shear crack (negative slab half), and (b) inside the shear crack

Further assumptions required for the calculation of the moment-rotation relationship according to the proposed model are the following:

1) The rotation of the slab is assumed to follow a sinusoidal law with maximum value ψ_{max} at 90° (tip of the negative slab half – Fig.3a) and minimum value ψ_{min} at 270° from the bending axis, as it is described in the following equation (angle φ measured from the bending axis):

$$\psi(\varphi) = \frac{\psi_{max} + \psi_{min}}{2} + \frac{\psi_{max} - \psi_{min}}{2} \cdot sin(\varphi) \tag{1}$$

2) No torsional moments are developed in the faces of the sector elements (rigid bodies).
3) The tangential moments are equal to the radial ones in the region inside the critical shear crack (Fig.3b).
4) The radius r_0 of the critical shear crack is equal to the eccentricity e.
5) The quadrilinear moment-curvature diagram that is assumed for concentric punching (Muttoni, 2008) is also adopted as the envelope for the extended model.

The mathematical expressions are presented hereafter. $M_{tan(\varphi-\Delta\varphi/2)}$ and $M_{tan(\varphi+\Delta\varphi/2)}$ are the integrals of the tangential moments at the faces of each sector element (Fig.3b). Subsequently these moments will be referred to as M_{tan}^- and M_{tan}^+, respectively, and are determined directly as a function of the assumed rotation, using the following formula (quadrilinear moment-curvature relationship):

$$M_{tan}(\varphi) = \big(m_R \cdot \langle r_y - r_0 \rangle + EI_1 \cdot \psi(\varphi) \cdot \langle ln(r_1) - ln(r_y) \rangle + EI_1 \cdot \chi_{TS} \cdot \langle r_1 - r_y \rangle \\ + m_{cr} \cdot \langle r_{cr} - r_1 \rangle + EI_0 \cdot \psi(\varphi) \cdot \langle ln(r_s) - ln(r_{cr}) \rangle \big) \tag{2}$$

where EI_0 and EI_1 are the stiffnesses before and after cracking, m_{cr} and m_R are the cracking moment and moment capacity respectively per unit width, χ_{TS} is the curvature due to the tension stiffening effect, and r_0, r_y, r_1, r_{cr} and r_s are the radii of the critical shear crack, of the yielded zone, of the zone in which cracking is stabilized, of the cracked zone and of the circular isolated slab element respectively. The operator $\langle x \rangle$ is x for $x \geq 0$ and 0 for $x < 0$. These parameters are the same as in CSCT (Muttoni, 2008). The only parameter that is updated for the case of seismically induced deformations is the radius r_0 of the critical shear crack (assumption 4) to take into account the fact that the shear force becomes less determinant as eccentricity increases. Therefore, the integral of the radial moment for a sector element at angle φ at $r = r_0$ is:

$$M_r(\varphi) = m_r(\varphi) \cdot r_0 \cdot \Delta\varphi \tag{3}$$

where $m_r(\varphi)$ is the radial moment per unit width at $r = r_0$ as function of the radial curvature (Muttoni, 2008).

If φ_i is the angle formed by the axis of bending and the bisector of the ith sector element, the shear force that can be carried by the compression strut of this sector element is derived by moment equilibrium in the tangential direction with respect to the centre of the column with radius r_c:

$$V_i \cdot \frac{\Delta\varphi}{2\pi} = \frac{1}{r_q - r_c}\left\{M_r(\varphi_i) + [M_{tan^+}(\varphi_i) + M_{tan^-}(\varphi_i)] \cdot \sin\left(\frac{\Delta\varphi}{2}\right)\right\} \qquad (4)$$

The total shear force acting on the connection for the load step k is:

$$V_k = \sum_{i=1}^{n} V_i \cdot \frac{\Delta\varphi}{2\pi} \qquad (5)$$

The moment equilibrium in the radial direction gives the torsional moment that is carried by the connection for the ith sector element:

$$M_{tor.r}(\varphi_i) = [M_{tan^+}(\varphi_i) - M_{tan^-}(\varphi_i)] \cdot \cos\left(\frac{\Delta\varphi}{2}\right) \qquad (6)$$

The different external loads acting on different sector elements provoke different moments for each load step k. The moment due to flexure (around the axis of the transferred moment) for the ith sector element is:

$$M_{flex.k}(\varphi_i) = V_i \cdot \frac{\Delta\varphi}{2\pi} \cdot (r_q - r_c) \cdot \sin(\varphi_i) \qquad (7)$$

The component of the torsional moment $M_{tor.r}(\varphi_i)$ that is parallel to the transferred moment for the ith sector element is:

$$M_{tor.k}(\varphi_i) = [M_{tan^+}(\varphi_i) - M_{tan^-}(\varphi_i)] \cdot \cos\left(\frac{\Delta\varphi}{2}\right) \cdot \cos(\varphi_i) \qquad (8)$$

The difference of compression forces of the strut along the shear crack between anti-diametric sector elements provokes moment due to shear force difference (Fig.4b). The component that is parallel to the bending axis is denoted as M_{ecc} and can be calculated using the following formula:

$$M_{ecc.k}(\varphi_i) = \left(V_i \cdot \frac{\Delta\varphi}{2\pi} - V_{i+n/2} \cdot \frac{\Delta\varphi}{2\pi}\right) \cdot r_c \cdot \sin(\varphi_i) \qquad (9)$$

Therefore, the total moment acting on the connection (parallel to the transferred moment) for the load step k is:

$$M_k = \sum_{i=1}^{n} M_{flex.k}(\varphi_i) + \sum_{i=1}^{n} M_{tor.k}(\varphi_i) + \sum_{i=1}^{n/2} M_{ecc.k}(\varphi_i) \qquad (10)$$

The total moment acting perpendicularly to the transferred moment is equal to zero ($M_{k.\perp} = 0$) and therefore global equilibrium is satisfied. The eccentricity calculated at load step k is:

$$e_k = M_k/V_k \qquad (11)$$

To obtain the relationship characterizing the flexural behaviour an iterative procedure should be adopted. The maximum rotation ψ_{max} is iterated so as to obtain the points that form the curve (denoted as load steps k) and the minimum rotation ψ_{min} is calculated to satisfy local and global equilibrium. For constant shear force V acting to the connection the iterative process for each load step terminates when $V_k \approx V$ so the moment-rotation curve is obtained and the radius r_0 of the shear crack is adapted at each load step.

As punching is a brittle local failure due to excessive shear stresses in the proximity of the slab-column connection, the need for a relationship between local rotations and global slab rotations ψ_{gl} becomes essential. At a global level, the rotation of the slab ψ_{gl} can be calculated as the average of the local rotations of the sector elements at the tip of the negative and positive slab half ψ_{max} and ψ_{min} respectively as follows:

$$\psi_{gl} = \frac{\psi_{max} + \psi_{min}}{2} \qquad (12)$$

The interstory drift rotation is related to the global slab rotation according to the following relationship:

$$\psi_{st} = \psi_{gl} + \psi_{col} \qquad (13)$$

where ψ_{col} is the contribution of the column deformation to the interstory drift.

GRAVITY LOAD EFFECT

EXPERIMENTAL INVESTIGATIONS

The influence of gravity loads on the stiffness, strength and deformation capacity of RC members subjected to lateral loading is often referred to as gravity load effect. The effect of gravity induced shear stresses on the behaviour and the strength of slab-column connections subjected to earthquake-type loading is rather significant. According to Pan and Moehle (1989) an increase of vertical load acting on a slab-column connection results in a decrease of stiffness, strength and rotation ductility. Although this affirmation is confirmed by numerous experimental campaigns (e.g. Pan and Moehle, 1989), there are others that show the inverse (e.g. Bu and Polak, 2009), i.e., an increase in stiffness and strength and partial enhancement of the rotation ductility when the gravity induced shear stresses are increased. In the following, the model presented in the previous section will be used to explain these different trends.

Table 1 summarises key parameters of eight tests by four groups of authors that investigated the gravity load effect by testing the same slab configuration under two different gravity shear ratios (GSR). These tests will be used to investigate why different groups of authors observed different trends. Next to the specimen size and the GSR the table summarises for each test the applied moment M_u at failure, the eccentricity e_u at failure ($e_u = M_u / V$), and the interstory drift $\psi_{st.u}$ at failure. The GSR is calculated as the vertical load acting on the connection divided by the punching resistance according to ACI 318 (2011) that is equal to $0.33 b_o d \sqrt{f_c'}$, where b_0 is the control perimeter located at $d/2$ from the face of the column, d the effective depth of the slab and f_c' the concrete compressive strength. The control perimeter is computed on the basis of straight corners.

6

Table 1. Parameters and results of tests represented in Fig.6 and Fig.7

Authors	Specimen size $2r_s$ (m)	Vertical load (kN)	GSR	e_u / r_s (-)	M_u (kNm)	$\psi_{st.u}$ (%)
Pan and Moehle (1989)	3.66	63 / 104	0.22 / 0.36	0.72 / 0.28	82 / 52	3.38 / 1.40
Choi et al. (2007)	2.40	81 / 150	0.30 / 0.50	0.84 / 0.38	81 / 68	2.67 / 3.00
Bu and Polak (2009)	1.50	110 / 160	0.53 / 0.68	0.86 / 0.66	70 / 78	2.79 / 2.69
Park et al. (2012)	2.70	132 / 159	0.44 / 0.41	0.40 / 0.34	71 / 74	1.24 / 1.37

GEOMETRY AND DEFORMATION CONSIDERATIONS

When analysing the tests displaying different trends, it was noticed that a key variable is the *e/L* ratio. Since r_s is a function of *L* and r_0 is assumed equal to *e*, the ratio r_0/r_s is directly related to *e/L*. For the same r_s and the same moment *M* transferred by the slab-column connection: An increase in *V* corresponds to a decrease in eccentricity *e* since *e=M/V*. Since $r_0=e$, the smaller the eccentricity, the larger the side faces of the sector elements and therefore the larger the tangential moment M_{tan} that is transferred via these faces (Eq. (2)). On the contrary, the smaller the eccentricity, the smaller the face formed by the critical shear crack and therefore the smaller the radial moment M_{rad} (Eq. (3)). This reasoning is based on the geometry of the sector element for a decrease of eccentricity, as illustrated in Fig.5.
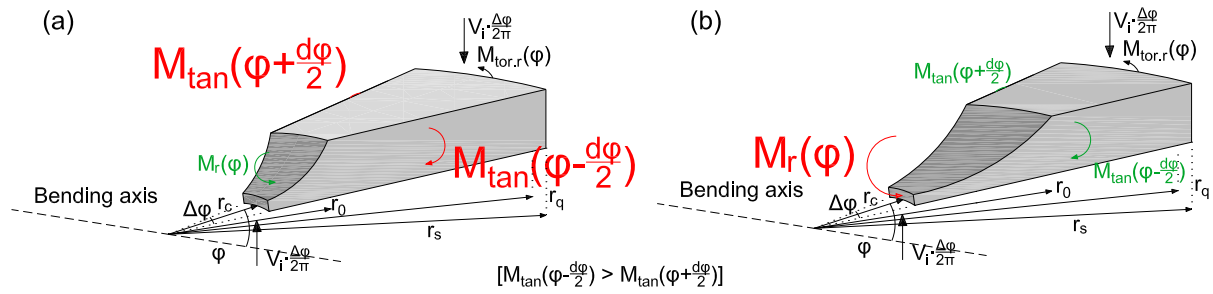

Figure 5. Influence of modified geometry on the sector element equilibrium components for (a) low eccentricity, and (b) high eccentricity

The deformation state of the slab is influencing the tangential moments that are developed in the side faces of the sector elements. The tangential moment per side face is calculated as the integral of the moment profile along the slab radius (Fig.3b and Eq.2). For an incremental rotation $\Delta\psi$ at both positive and negative slab half the radii r_y, r_1 and r_{cr} decrease and increase by the same length Δr respectively, as they are proportional to ψ (Muttoni, 2008). The resulting tangential moment increment ΔM_{tan} due to the variation by Δr of the radii r_y, r_1 and r_{cr} results from the part of the sector outside the radius r_y, i.e., $r_s - r_y$ (Fig.3b) and therefore the smaller $r_s - r_y$ the smaller is the tangential moment increment ΔM_{tan}. With an increase in *V* the radius r_y where overall reinforcement yielding occurs increases and therefore the radius $r_s - r_y$ decreases. Consequently the increase of the tangential moment ΔM_{tan} for the same rotation difference $\Delta\psi$ is smaller than for a case with less vertical load. Therefore, the behaviour under increased *V* becomes softer.

For the same *e* the geometry of the sector elements is not modified and to assess the effect of an increase of r_s only the deformation state of the slab is considered. For the same *e* and *M* the vertical load *V* is the same (since *e=M/V*) and therefore the tangential moment M_{tan} increases to compensate the increase of the lever arm $r_q - r_c$ (Eq.4). So the rotation of the slab increases and the behaviour becomes softer.

GRAVITY LOAD EFFECT AS FUNCTION OF r_0/r_s

For large values of r_0/r_s the geometry of the sector elements is more important than the specimen size. An increase in V provokes an increase of rotations rendering the increase of the tangential moment M_{tan} more important and the decrease of the radial moment M_{rad} less important. Therefore, for an increase in V the behaviour becomes stiffer. On the contrary, for low values of r_0/r_s the geometry of the sector elements becomes less important than the specimen size. For these cases an increase in V results in a softer behaviour.

The gravity load effect for low values of r_0/r_s is illustrated in Fig.6. The gravity load effect for large values of r_0/r_s is illustrated in Fig.7a. The two aforementioned effects tend to cancel each other out when the comparison is performed at intermediate values of r_0/r_s, as shown in Fig.7b.
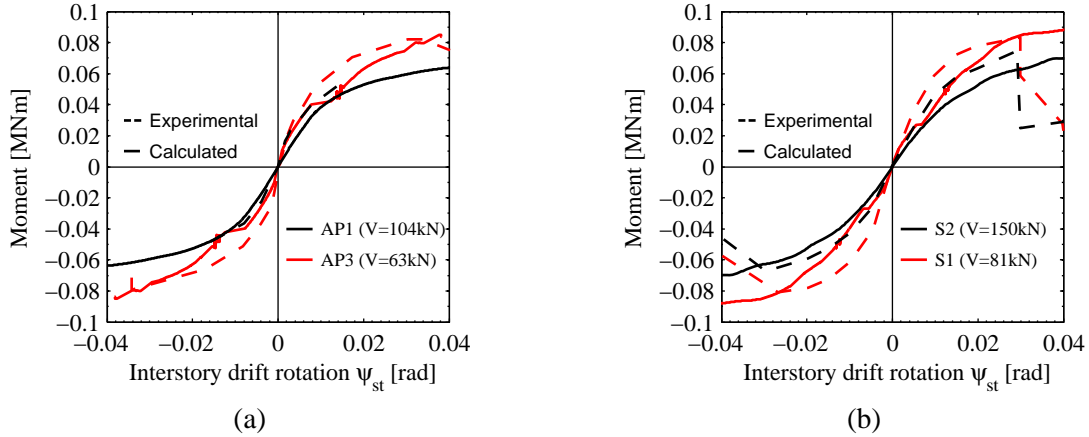

(a)   (b)

Figure 6. Gravity load effect for isolated specimens with low values of r_0/r_s at failure: (a) Pan and Moehle (1989), and (b) Choi et al. (2007)

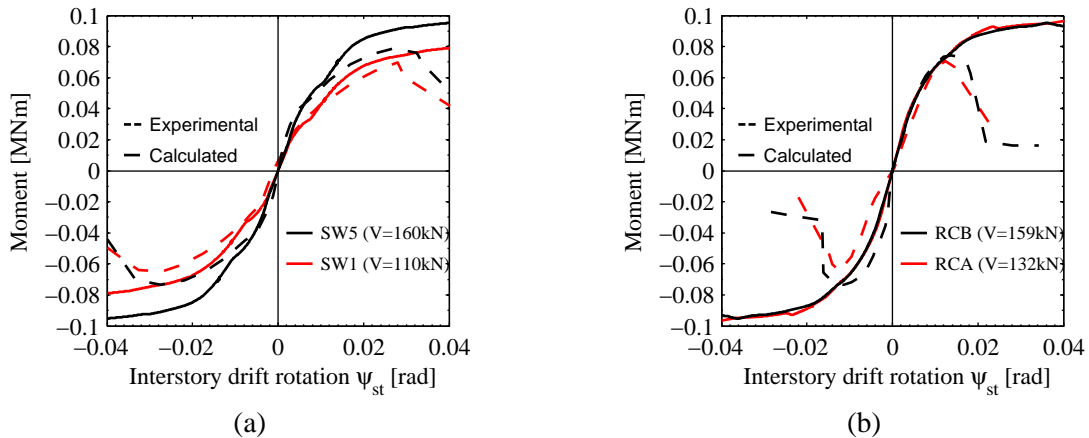(a)   (b)

Figure 7. Gravity load effect for isolated specimens (a) with low values of r_0/r_s at failure (Bu and Polak, 2009), and (b) intermediate values of r_0/r_s at failure (Park et al., 2012)

PARAMETRIC ANALYSES

To support these findings, Fig.8 shows calculated moment-rotation curves for various vertical loads for configurations identical to the specimens tested by Pan and Moehle (1989) and Bu and Polak (2009). In Fig.8a the red and black color curves represent the vertical load levels adopted by Pan and Moehle (1989), 60 kN and 100 kN respectively. As can be seen from the green curve ($V = 40$kN), if a smaller vertical load V had been chosen the behaviour for high values of r_0/r_s would be softer comparing to higher vertical loads. In Fig.8b the red and blue color curves represent the vertical load levels chosen by Bu and Polak (2009), 100 kN and 150 kN respectively. If the adopted vertical load V

had been higher (black color curve corresponding to $V = 200$ kN), the moment-rotation relationship would have been softer.
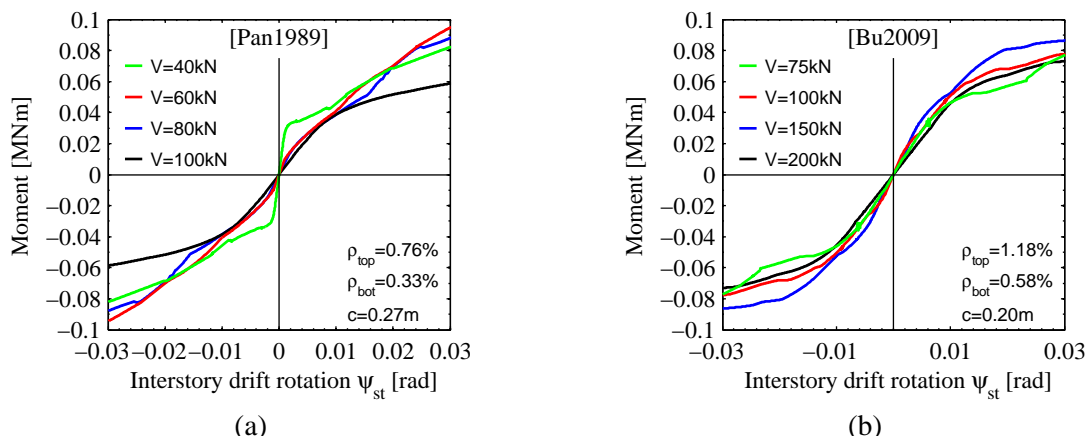

(a) (b)

Figure 8. Influence of vertical loading on the flexural response of slab-column connections under seismic loading: (a) Pan and Moehle (1989), and (b) Bu and Polak (2009)

These considerations have considerable implications for the earthquake-resistant design of flat slab buildings with relatively short spans. As the primary aim of increasing the number of columns is the reduction of the vertical load carried by each slab-column connection, the eccentricity e increases. Moreover, for shorter spans the span length L decreases and consequently r_s decreases as well. Therefore, the ratio r_0/r_s increases and, as shown before, decreased vertical loads appear to confer lower moment capacity. Thus, for the earthquake-resistant design of flat slab buildings with relatively short spans it is rather unsafe to consider low vertical loads, contrary to the earthquake-resistant design of flat slab buildings with medium and large spans.

As shown above the gravity load effect on the flexural behaviour of slab-column connections is effectively captured by the analytical model proposed by the authors. Moreover, it allows to explain why for some configurations an increase in gravity loads results in a stiffer behaviour. The model shows that the key variable is the ratio r_0/r_s, i.e., the ratio of eccentricity to specimen size.

LATERAL FORCE RESISTING MECHANISMS

A realistic estimation of the contribution of the resisting mechanisms to the overall capacity of the slab-column connection is rather difficult because of the non-linear behaviour of the slab-column connection and the fact that the externally applied bending moment is resisted by three different mechanisms (eccentric shear force, flexure and torsion). The design approaches in codes of practice (ACI 318, 2011; Eurocode 2, 2004) are based on estimating the contribution of the eccentric shear and bending moment mechanisms on the basis of experiments and empirical works while neglecting the contribution of the torsion mechanism. This approach presents however several shortcomings, the most important being the fact that the distribution of shear stresses on the critical perimeter is in reality not linear as assumed in the model. Furthermore, the contribution of eccentric shear force and flexure mechanisms is constant for any drift level, equal to 40% and 60% respectively for square columns according to ACI 318 (2011). This is not representative of the actual behaviour of slab-column connections under increasing lateral deformations as results of the analytical model will show.

The analytical model allows to predict the contribution of all resistance-providing mechanisms at any drift level. The results are illustrated for the tests conducted by Pan and Moehle (1989) in Fig.9 and for the tests by Bu and Polak (2009) in Fig.10. For those two test series the analytical model yields rather accurate predictions of the moment-rotation curve, as shown in the previous section.
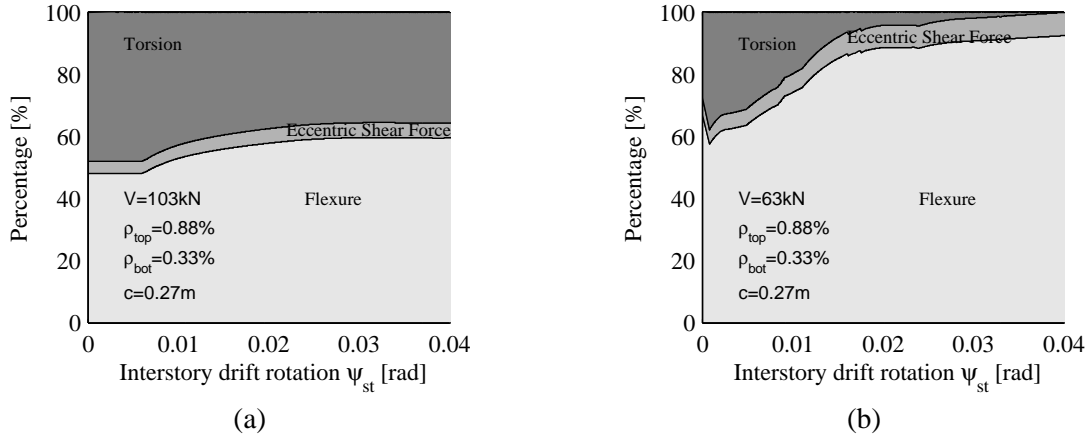
Figure 9. Mechanisms contributing to the lateral resistance of slab-column connections for large specimens as function of the interstory drift for (a) high vertical loads and (b) low vertical loads

As can be seen from Fig.9 and Fig.10 the contribution of the mechanisms of flexure, eccentric shear force and torsion depends strongly on the drift level as well as on the vertical load acting on the slab. For relatively low vertical loads, the torsion contribution is decreasing much more rapidly for increasing values of drifts (Fig.9b) when compared to high vertical loads (Fig.9a). This is due to the modified geometry of the sector elements for high eccentricity (see previous section). As the radius r_0 is increasing the slab region outside the shear crack decreases and consequently the unequal tangential moments that provoke the torsion transfer (Eq.8) are decreasing. Likewise, the contribution of flexure becomes more important for increasing drifts, in particular for high eccentricities. Furthermore, higher eccentricities result in larger contribution of the eccentric shear force mechanism.
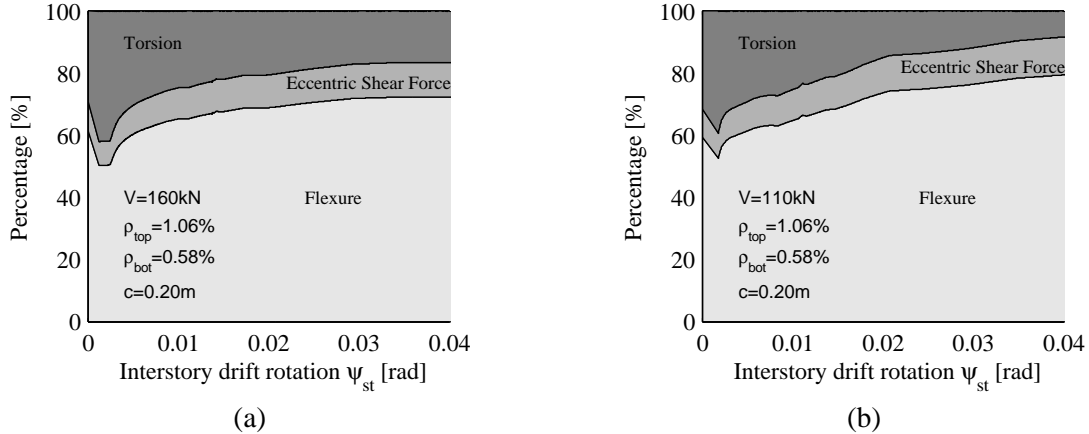

Figure 10. Mechanisms contributing to the lateral resistance of slab-column connections for small specimens as function of the interstory drift for (a) high vertical loads and (b) low vertical loads

From Fig.9 and 10, when comparing the contribution of the various mechanisms for specimens with approximately equal vertical loads, it is observed that for shorter specimens (Fig.10b) the torsion contribution is decreasing much more rapidly than for larger ones (Fig.9a). It should be noted that the unequal tangential moments of each sector element that provoke the torsion in the connection are smaller for smaller specimen sizes as the region outside the shear crack becomes smaller. Moreover, the sensitivity of a small specimen to an increase of eccentricity provokes much more rapidly a decrease of tangential moments than for a relatively large specimen.

The presented approach yields hence new insights into the performance of approaches included in codes of practice for predicting the ultimate moment of slab-column connections under earthquake loading. The assumption that the flexure mechanism contribution is approximately equal to 60% of the total moment inserted in the connection (ACI 318, 2011) seems rather accurate for relatively low drifts whereas for higher drift values it is underestimating the actual contribution of the

flexural mechanism to the overall resistance. The latter results in an overestimation of the contribution of the eccentric shear force mechanism. As the total moment capacity is calculated using the shear stress criterion, the resulting predictions are conservative.

CONCLUSIONS AND OUTLOOK

An analytical approach for estimating (i) the contribution of all resistance-providing mechanisms of RC slab-column connections as well as (ii) the moment-rotation relationship of RC slab-column connections under seismically induced deformations is presented. The model is based on the Critical Shear Crack Theory and can effectively uncouple the contribution of the various resisting mechanisms (flexure, eccentric shear force and torsion) when a slab-column connection is subjected to earthquake-induced deformations.

The decreasing lateral stiffness of slab-column connections with increasing vertical loads is verified for experiments with small ratios of eccentricities to the specimen size. For high ratios of eccentricities to specimen size the increasing lateral stiffness of slab-column connections with increasing vertical loads is also predicted and theoretically explained. Therefore, the gravity load effect for slab-column connections depends on the eccentricity level and the column-to-column distance.

In terms of the contribution of the different resisting mechanisms it is shown that for small values of drifts the flexural mechanism is carrying about 60% of the total resisting moment as prescribed by ACI 318 (2011). Nevertheless, under decreasing vertical loads the flexure mechanism is rapidly increasing for increasing values of drifts whereas the contribution of torsion is rapidly decreasing. Moreover, for relatively small specimen sizes the contribution of torsion is found to decrease much more rapidly than for large specimens.

An ongoing experimental campaign will provide more insight into the behaviour of slab-column connections under increasing vertical loads. Moreover, it is anticipated that these new tests will offer a better understanding of the contribution of resistance-providing mechanisms and of the parameters that are influencing the failure criterion. Other aspects, such as the influence of cyclic loading as well as the column size effect will also be investigated.

REFERENCES

ACI 318 (2011) "Building code requirements for structural concrete (ACI-318-11) and commentary (ACI 318R-11)", *American Concrete Institute*, Farmington Hills, USA

Bu W and Polak AM (2009) "Seismic Retrofit of Reinforced Concrete Slab-Column Connections Using Shear Bolts", *ACI Structural Journal*, 106(4):514-522

Choi MS, Cho IJ, Han BS, Ahn JM, Shin SW (2007) "Experimental Study of Interior Slab-Column Connections Subjected to Vertical Shear and Cyclic Moment Transfer", *Key Engineering Materials*, 348-349:641-644

Drakatos IS, Muttoni A, Beyer K (2014) "Mechanical Model for Flexural Behaviour of Slab-Column connections under Seismically induced Drifts", *Proceedings of the 4th fib Congress*, Mumbai, India, 10-14 February 2014, 639-642

Eurocode 2 (2004), "Design of concrete structures – Part 1-1: General rules and rules for buildings", *CEN, EN 1992-1-1*, Bruxelles, Belgium.

fib Bulletin 56 (2010), "Model code 2010 – First complete draft", *Fédération internationale du béton (fib)*, Lausanne, Switzerland

Kanoh Y and Yoshizaki, S (1979) "Strength of slab-column connections transferring shear and moment", *ACI Journal*, 76(2):461-478

Hanson NW and Hanson JM (1968) "Shear and moment transfer between concrete slabs and columns", *Journal of the Portland Cement Association*, 10(1):2-16

Muttoni A (2008) "Punching shear strength of reinforced concrete slabs without transverse reinforcement", *ACI Structural Journal*, 105(4):440-450

Pan A and Moehle JP (1989) "Lateral Displacement Ductility of reinforced concrete flat plates", *ACI Structural Journal*, 86(3):250-258

Park HG, Kim YN, Song JG, Kang SM (2012) "Lattice Shear Reinforcement for Enhancement of Slab-Column Connections", *Journal of Structural Engineering ASCE*, 128(3):425-437